

## **STRUCTURAL CHARACTERISTICS OF Sodium Calcium Silicate Glass Ceramics**

Than Min Khaing<sup>1</sup>, Min Maung Maung<sup>2</sup>, Yee Mon Tun<sup>3</sup>

### **Abstract**

Glass ceramics were prepared by the sol-gel method using sodium metasilicate ( $\text{Na}_2\text{SiO}_3$ ) as a silica source. The obtained samples were sintered at three different temperatures (800°C, 900°C, and 1000°C). The presence of sodium calcium silicate was observed by an X-ray diffraction (XRD) pattern. The major phase formation of combeite ( $\text{Na}_2\text{Ca}_2\text{Si}_3\text{O}_9$ ) and the secondary phase formation were also observed. The optical band gap of this sample was investigated with the help of a UV-vis spectrophotometer. The optical band gaps were found to be in the range of 4.7 eV – 4.92 eV. The Fourier Transform Infrared (FTIR) spectroscopy was employed for the characterization of these materials.

**Keywords:** Glass Ceramics, Sol-Gel, XRD, UV-vis and FTIR

### **Introduction**

The field of biomaterials began to shift emphasis from achieving exclusively a bioinert tissue response to producing bioactive components that could have a controlled action and reaction in the physiological environment. Biomaterials have recently been improved for new medical applications (Abbasi and Hashemi 2014). The original bioactive glass was first discovered in 1970 by Larry L. Hench. Its composition consists of 45 %  $\text{SiO}_2$ , 24.5 %  $\text{CaO}$ , 24.5 %  $\text{Na}_2\text{O}$ , and 6.0 %  $\text{P}_2\text{O}_5$  (wt. %, noted as 45S5) (Dang et al. 2020). Peitl et al. have developed the first bioactive glass-ceramic in the  $\text{SiO}_2$ - $\text{CaO}$ - $\text{Na}_2\text{O}$ - $\text{P}_2\text{O}_5$  system with both good mechanical properties and high bioactivity. After that, Ravagnani et al. developed a highly bioactive, fully crystalline glass-ceramic in the  $\text{SiO}_2$ - $\text{CaO}$ - $\text{Na}_2\text{O}$ - $\text{P}_2\text{O}_5$  system. Almost all the works have shown that  $\text{Na}_2\text{Ca}_2\text{Si}_3\text{O}_9$  formation, observed in some glass-ceramics, enhances the mechanical properties of the starting glass and maintains the high bioactivity of particular compositions in the  $\text{SiO}_2$ - $\text{CaO}$ - $\text{Na}_2\text{O}$ - $\text{P}_2\text{O}_5$  system (Mezahi et al. 2018). Recently, calcium silicate based glass ceramics have been regarded as a potential candidate for bone replacement and regeneration due to their excellent biocompatibility and bioactivity. Controlled surface crystallization of calcium silicate glass ceramics develops such versatile mechanical properties that it can be utilized as a dental implant or as a coating for an implant (Mirza et al. 2017). Bonding between bioactive glass-ceramic and the surrounding tissues takes place through the formation of a hydroxyapatite layer, which is very similar to the mineral phase of bone (Kumar n.d.). One of the more interesting methods to synthesize organic-inorganic hybrid materials at low temperature is the sol-gel technique. Two important reactions are involved; in fact, in this chemical synthesis, the precursor undergoes hydrolysis to form a colloidal suspension (sol), followed by a condensation reaction that allows “sol” evolution into “gel” (Fernandes et al. 2018). Generally, sol-gel-derived glass, with its inherent mesoporosity, provides a larger surface area and consequently a more rapid degradation rate than melt-derived glass of similar composition (Gmeiner et al. 2015). Nevertheless, different results found in the literature show that not just composition but also the preparation method influence on the final structure and the resultant biological properties of the material (Quintero Sierra and Escobar 2019). In this study, glass ceramics powder in a quaternary system was synthesized through the sol-gel route using sodium metasilicate as a cheap silica source. The synthesized glass ceramics were analyzed by X-ray diffraction (XRD). The optical band gap of the glass ceramic powder was characterized by Ultraviolet visible spectrophotometer (UV-vis). The functional groups of the glass ceramics powders were analyzed by Fourier Transfer Infrared (FTIR) spectroscopy.

---

<sup>1</sup>Department of Physics, Patheingyi Education Degree college

<sup>2</sup>Department of Physics, University of Yangon

<sup>3</sup> Department of Physics, Government of Technical Institute (Insein)

## Materials and methods

### Experimental procedures

Glass ceramics were synthesized through the sol-gel process from sodium metasilicate,  $\text{Na}_2\text{SiO}_3$  according to the following procedure. The  $\text{Na}_2\text{SiO}_3$  was stirred in a beaker using a magnetic stirrer in deionised water followed by addition of ethanol to give a clear solution. To the stirred mixture was added 1M  $\text{HNO}_3$  drop wise, stirring was continued further for 1 h to allow complete hydrolysis.  $\text{P}_2\text{O}_5$  and  $\text{Ca}(\text{NO}_3)_2 \cdot 4\text{H}_2\text{O}$  were added in sequence under constant stirring. Each reagent was allowed 45 min to react before adding the next reagent, finally the mixture was stirred for 1 h after the last addition. The resulting gel was aged at room temperature for 5 days, dried at  $60^\circ\text{C}$  for 72 h. The resulting glass ceramics were sintered at  $800^\circ\text{C}$ ,  $900^\circ\text{C}$  and  $1000^\circ\text{C}$  for 2 h. The sintered specimen was analyzed by X-ray diffraction (XRD) using  $\text{CuK}\alpha$  radiation source operated at 40 kV and 30 mA. The diffraction patterns were obtained in the  $2\theta$  range from  $10^\circ$ - $70^\circ$ . The obtained glass ceramics were investigated with UV-vis spectroscopy. The functional groups of the materials were studied by FTIR spectroscopy.

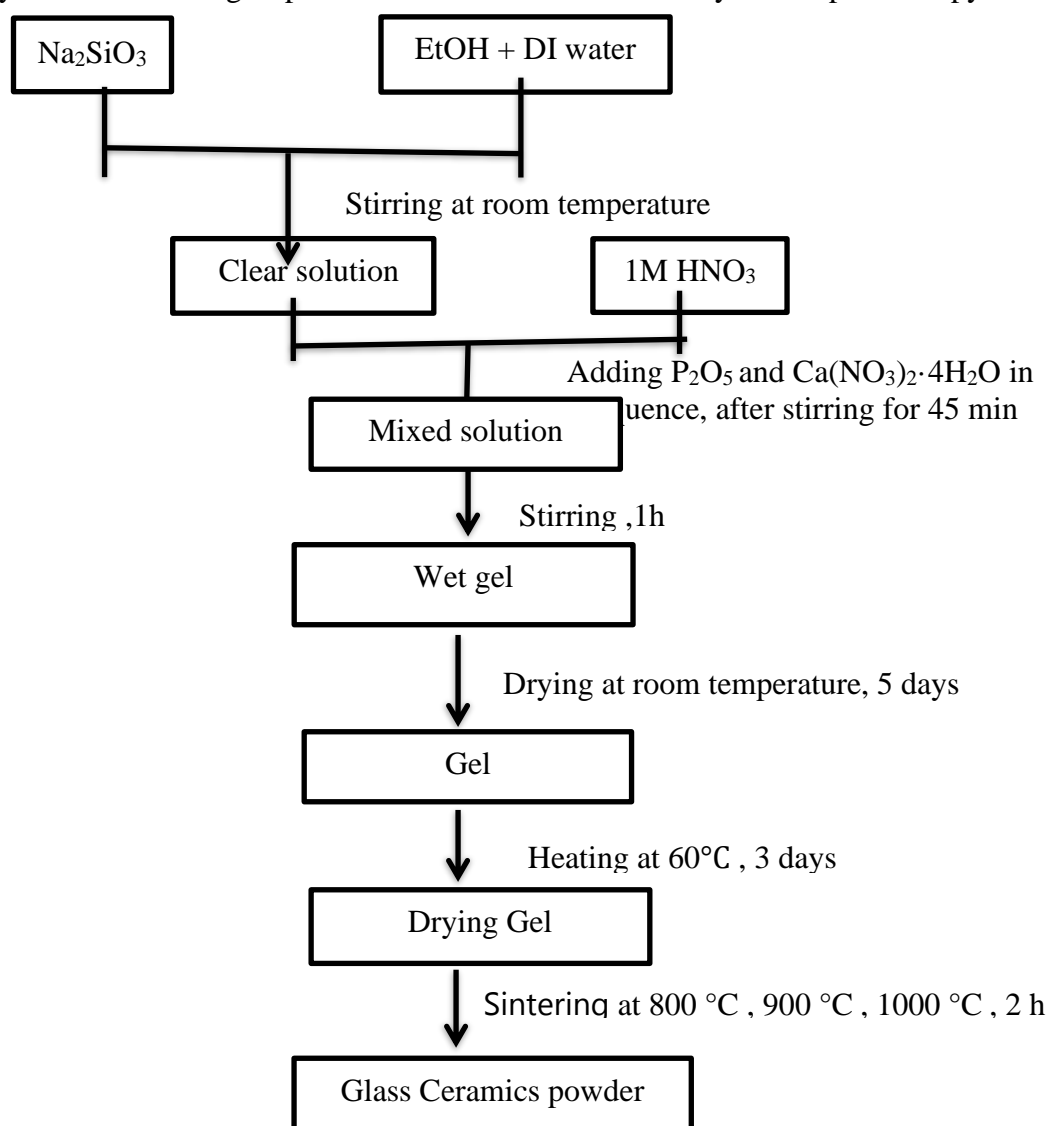


**Figure.1** Block diagram of the preparation of glass ceramics

## Results and Discussion

### X-Ray Diffraction Analysis

The XRD patterns containing crystalline peaks Fig. 2 (d) were used to obtain the crystalline size of combeite at various heat treatment temperatures using the Scherrer equation (Patterson 1939).

$$D = \frac{k\lambda}{\beta \cos\theta} \quad (1)$$

In this formula,  $\lambda = 0.154056$  nm presents the wavelength of  $\text{CuK}\alpha$ ,  $\beta$  is for the full width at half maximum ( FWHM ),  $k$  is the Scherrer's constant, which is taken as 0.9 , and  $\theta$  stands for the diffraction angle. In figure 2(d), the intensity of the peaks was a good match to the standard PDF # 96-900-7712, indicating the formation of the crystalline phase of  $\text{Na}_2\text{Ca}_2\text{Si}_3\text{O}_9$ . This peak shows agreement with the results from several other researchers (Aswad, Sabree, and H S Abd 2021). Above a sintering temperature of 800 °C, 45S5 starts to crystallize, forming mainly the  $\text{Na}_2\text{Ca}_2\text{Si}_3\text{O}_9$  crystalline phase (Kaur et al. 2019). With increasing sintering temperature, the intensity of the peaks increases, and the diffraction peaks become sharper and narrower. This indicates the enhancement of the crystalline nature and an increase in the crystallite size. Peaks in the  $2\theta$  range from  $33^\circ$ – $35^\circ$ , with the corresponding Miller Indices (220), are more intense compared to the remaining peaks across all the samples. This occurs because crystal planes orient along a specific direction over a long-range, leading to a preferred crystallographic orientation. Low-intensity peaks indicate, the random arrangement of the crystals. Thus it could be concluded that the size of the combeite crystals increased up to 33.2 nm by increasing the heat treatment temperature from 800 °C to 1000 °C . The crystallite sizes of combeite calculated using eq. (1) and the XRD patterns of Fig. 2(d) are summarized in table.

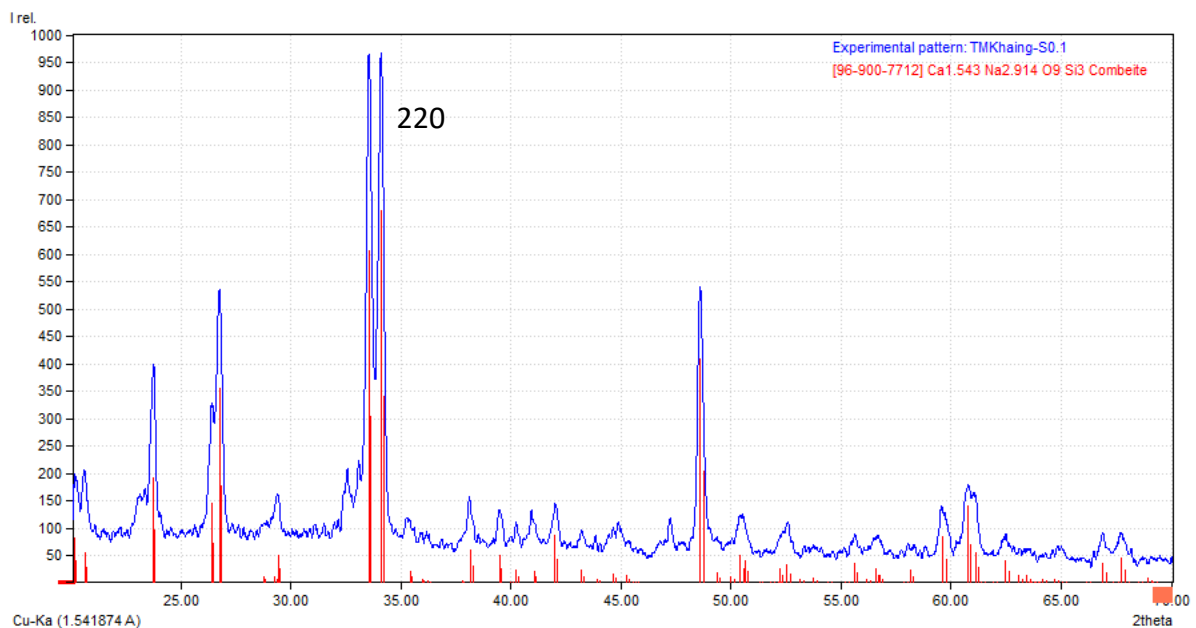


**Figure- 2(a)** XRD pattern of the glass ceramics sintered at 800 °C for 2 h .

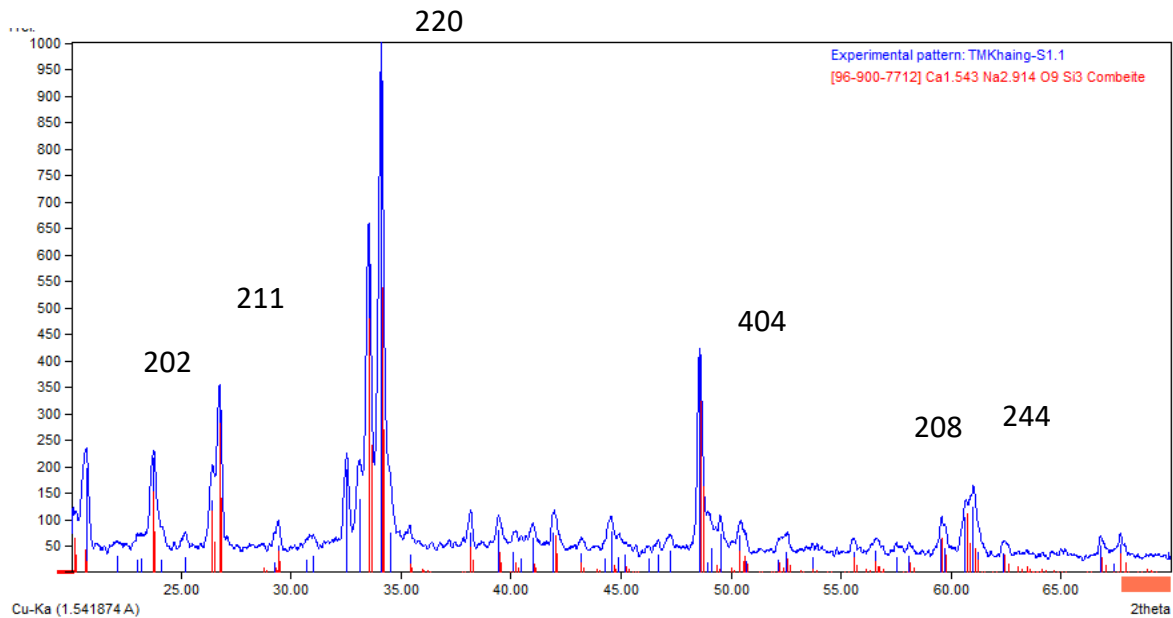


**Figure- 2(b)** XRD pattern of the glass ceramics sintered at 900 °C for 2 h

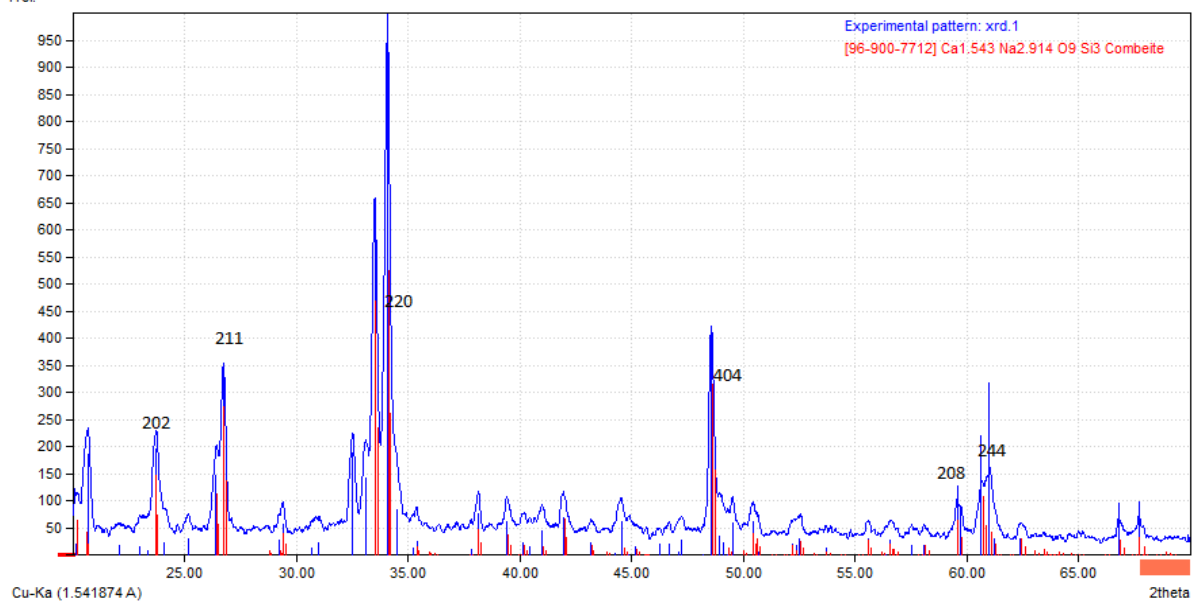


**Figure- 2 (c)** XRD pattern of the glass ceramics sintered at 1000 °C for 2 h .

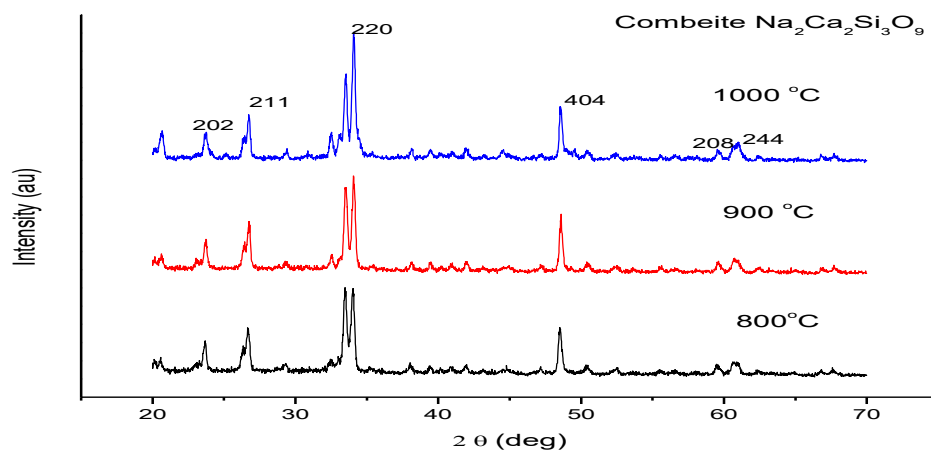


**Figure- 2 (d)** XRD pattern of the glass ceramics sintered at 1000 °C , 900 °C and 800 °C for 2 h .

**Table – The crystallite sizes of the combeite (Na<sub>2</sub>Ca<sub>2</sub>Si<sub>3</sub>O<sub>9</sub>) samples at various temperature.**

Heat treatment temperature (°C)	800	900	1000
Crystallite sizes (nm)	31.2	31.7	33.2

**UV-Vis Analysis**

The absorption spectrum and the energy band gap of glass ceramics were measured using a UV-vis spectrometer (PerkinElmer) in the Department of Physics, Yangon University. The energy band gap value  $E_g$  could be determined by analyzing the optical data with the optical absorption coefficient  $\alpha$  and the photon energy  $h\nu$  using Tauc’s relation,  $(\alpha h\nu)^2 = A(h\nu - E_g)$ . The optical absorption spectra were recorded at room temperature in the range of wavelengths from 202 nm to 1100 nm. The optical band gap was evaluated by plotting  $(\alpha h\nu)^2$  vs  $h\nu$  as shown in Figure 3(a-c) . Extrapolating the linear portion of the absorption edge  $(\alpha h\nu)^2$  the photon energy axis gives the direct energy band gap of the glass ceramics. The band gap energies (eV) for the combeite (Na<sub>2</sub>Ca<sub>2</sub>Si<sub>3</sub>O<sub>9</sub>) are 4.7 eV, 4.82 eV, and 4.91 eV, respectively. The values for  $E_g$  of the glass–ceramic samples show an increase as the heating temperature increase gradually(Kolli, Kanikaram, et al. 2022). The results of this study indicate that combeite could be employed in optoelectronic devices (Zosiamliana et al. 2022).

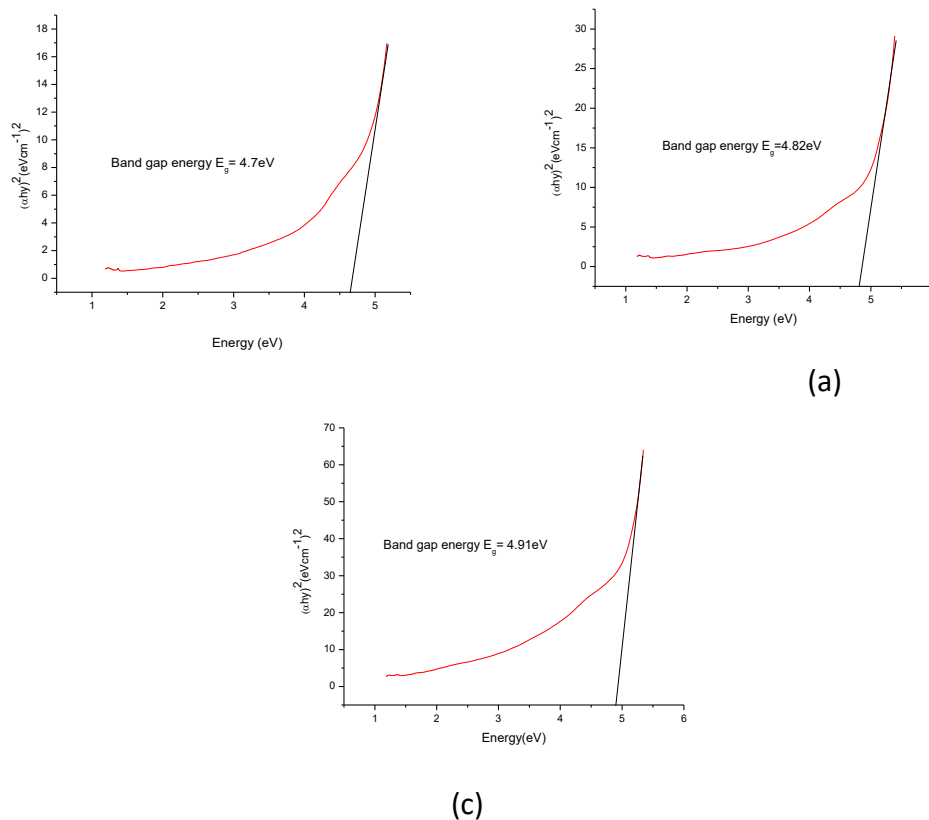


**Figure - 3** The energy band gap values of combeite (Na<sub>2</sub>Ca<sub>2</sub>Si<sub>3</sub>O<sub>9</sub>) at (a) 800 °C, (b) 900 °C and (c) 1000 °C .

**Fourier - transform infrared (FTIR) Analysis**

The information from the infrared spectra of the samples can be used to investigate and gain additional information and data regarding the existence of different structural groups in the

materials. Fig. 4(a-c) shows the FTIR spectrum of the glass–ceramics within the range of  $400\text{ cm}^{-1}$  and  $4000\text{ cm}^{-1}$  sintered at different temperatures. The bands in the low-frequency range around  $400\text{ cm}^{-1}$ – $600\text{ cm}^{-1}$  can be attributed to the vibration of Si–O bonding. The mid-frequency band between  $600\text{ cm}^{-1}$  to  $800\text{ cm}^{-1}$  can be associated with and related to the presence of Si–O and Si–O–Si bond bending symmetric stretching vibrations in the sample. Besides, the higher frequency band within the spectral range  $800\text{ cm}^{-1}$  to  $1250\text{ cm}^{-1}$  can be related to the Si–O bond inwards the  $\text{SiO}_4$  tetrahedron asymmetric stretching modes (Zaid et al. 2020). The  $447\text{ cm}^{-1}$ ,  $449\text{ cm}^{-1}$  and  $451\text{ cm}^{-1}$  peaks are assigned to Si-O-Si bending vibration, which is attributed to normal vibration modes of Si-O in the  $\text{SiO}_4$  group, indicating the presence of amorphous silicate. The absorption bands at  $574\text{ cm}^{-1}$  and  $576\text{ cm}^{-1}$  can be assigned to O-P-O bending vibrations of bridging phosphorous, and the one at  $518\text{ cm}^{-1}$  to O=P-O vibrations (Gavinho et al. 2021). The band at  $621\text{ cm}^{-1}$  and  $698\text{ cm}^{-1}$  confirmed that the presence of cristobalite phase in glass ceramics and it was most likely arising from the sodium calcium silicate phase. The broad peaks at  $923\text{ cm}^{-1}$  and  $931\text{ cm}^{-1}$  indicate the presence of Si-O-Ca vibrations. Similar values were observed for other cyclo-silicates (Kolli, V M, et al. 2022). The spectra at  $1031\text{ cm}^{-1}$ ,  $1033\text{ cm}^{-1}$  and  $1039\text{ cm}^{-1}$  showed a strong absorption band of Si-O-Si asymmetric stretching vibration. The peak is located at  $1446\text{ cm}^{-1}$  due to the presence of carbonate ( $\text{CO}_3^{2-}$ ). The presence of carbonate bonds is attributed the a carbonation process of the material due to the atmospheric  $\text{CO}_2$  as a consequence of the high calcium content in the preparation. The high  $\text{Ca}^{2+}$  content also causes the formation of a band at  $1483\text{ cm}^{-1}$ . The band at  $2852\text{ cm}^{-1}$  and  $2924\text{ cm}^{-1}$  were assigned the symmetric and asymmetric stretching vibrations of C-H bonding. The broad peak centered at  $3400\text{ cm}^{-1}$ ,  $3442\text{ cm}^{-1}$  and  $3452\text{ cm}^{-1}$  and the peak at  $1637\text{ cm}^{-1}$  and  $1653\text{ cm}^{-1}$  are ascribed to the stretching and bending vibrations of the O-H group in adsorbed water molecules. These bands were present in the sintered samples because the water molecules were unable to escape from the silica matrix.

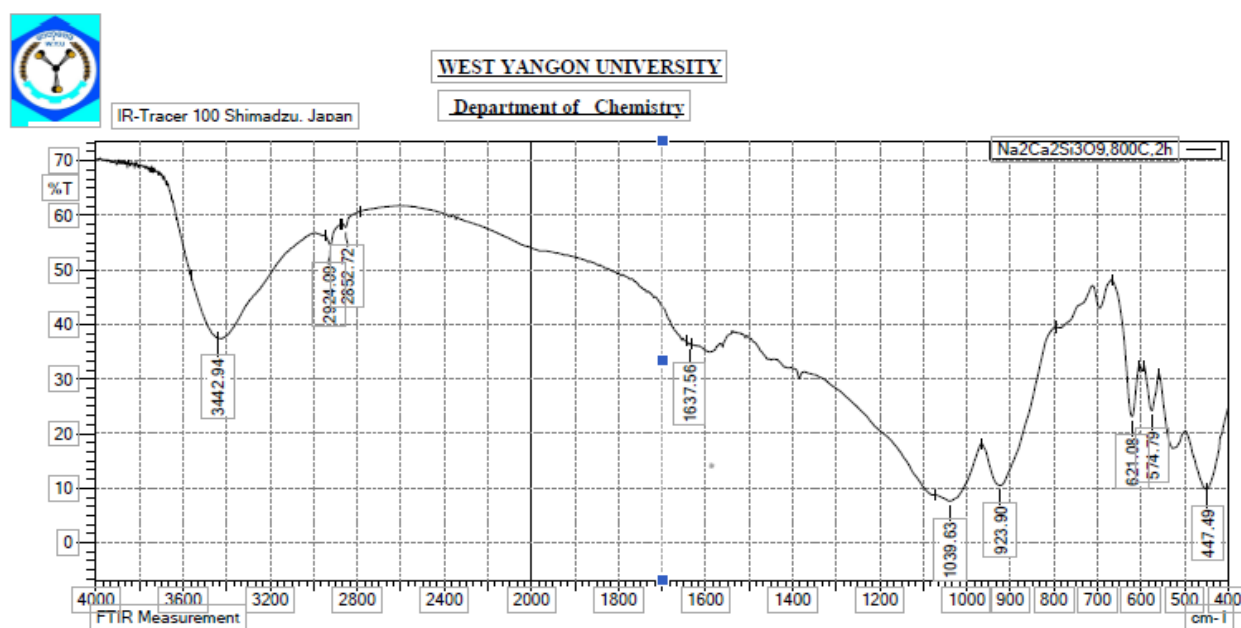


**Figure-4 ( a )** FTIR spectrum the synthesized combeite heat treated at  $800\text{ }^{\circ}\text{C}$

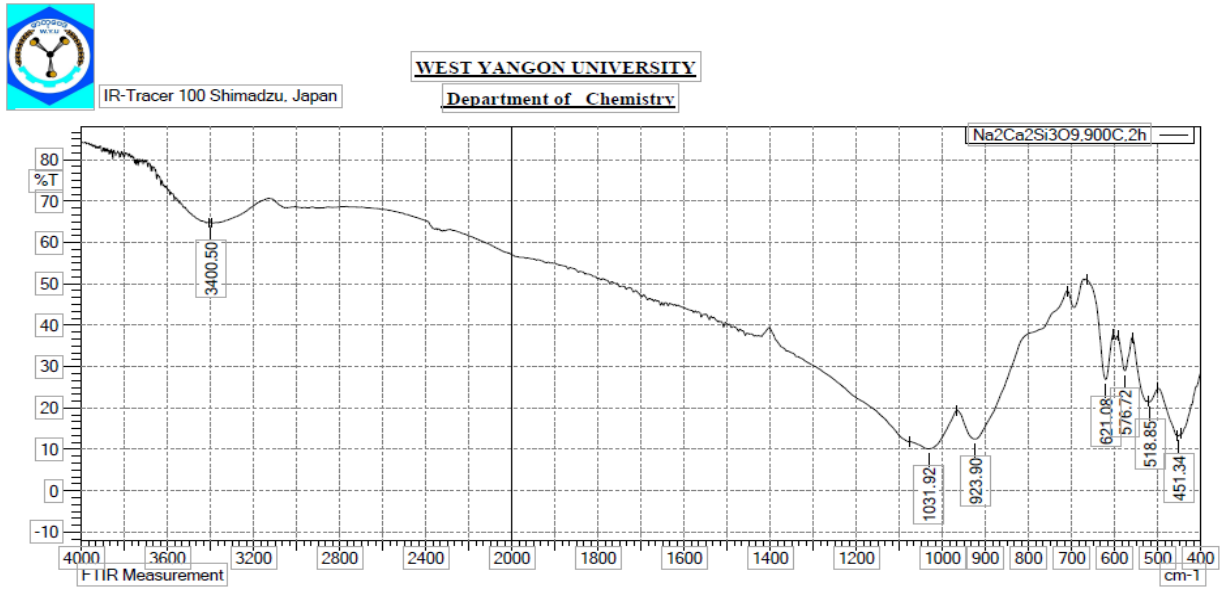


Figure-4 ( b) FTIR spectrum the synthesized combeite heat treated at 900 °C

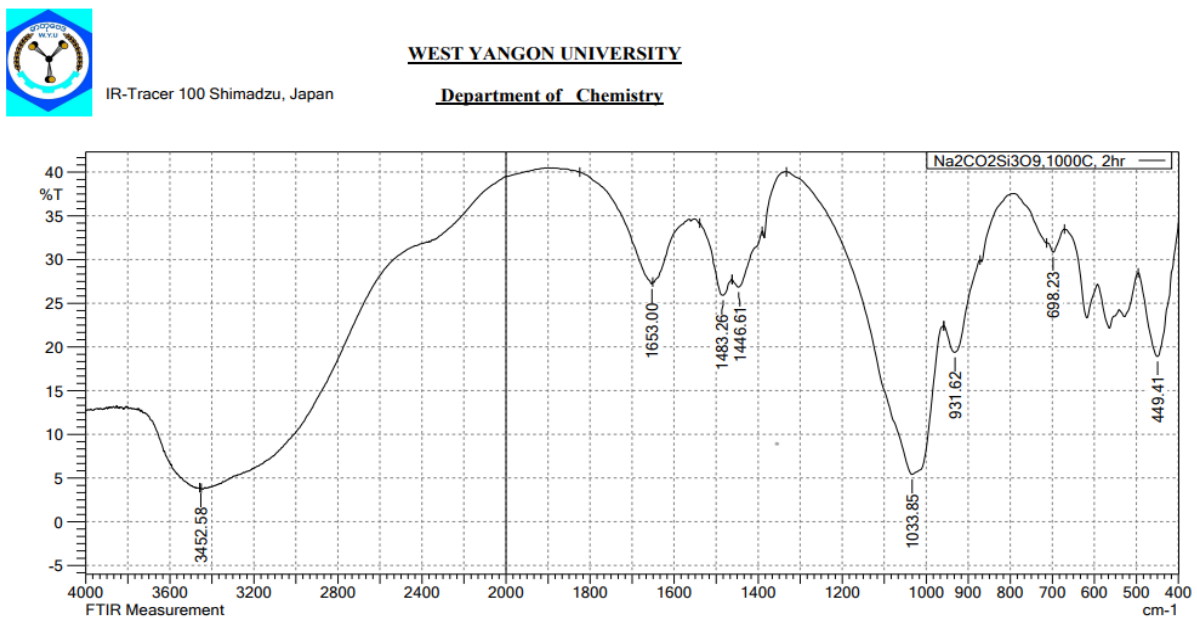


Figure-4 ( c) FTIR spectrum the synthesized combeite heat treated at 1000 °C

### Conclusion

SiO<sub>2</sub>-CaO-Na<sub>2</sub>O-P<sub>2</sub>O<sub>5</sub>-based glass ceramics were synthesized through the sol-gel process using sodium metasilicate as a silica precursor. Extensive thermal treatments and characterizations reveal that the optimized protocol could be employed to produce pure combeite at temperatures between 800 °C – 1000 °C. The X-ray diffraction (XRD) patterns of the glass-ceramics show the presence of crystalline phases of sodium calcium silicate, Na<sub>2</sub>Ca<sub>2</sub>Si<sub>3</sub>O<sub>9</sub>. The secondary phase formatting may be P<sub>2</sub>O<sub>5</sub> phase. This phase was confirmed by FTIR results. From the optical studies, the optical band gaps were estimated to be in the range of 4.7 eV – 4.91 eV. In the presented spectrum, the absorption bands of silicate groups were clearly evident. This spectrum was indicated high surface area silica structures.

## Acknowledgements

The authors would like to express our deepest gratitude to the Department of Physics and Universities' Research Center, University of Yangon, for the supports with research facilities. The author is grateful to Dr Nu Nu Aye, Principle, Patheingyi Education Degree College, for her kind encouragement and permission. We deeply thank the Myanmar Academy of Arts and Science for submission of research paper.

## References

- Abbasi, Mojtaba, and Babak Hashemi. 2014. "Fabrication and Characterization of Bioactive Glass-Ceramic Using Soda-Lime-Silica Waste Glass." *Materials Science and Engineering C* 37(1): 399–404. <http://dx.doi.org/10.1016/j.msec.2014.01.031>.
- Aswad, M A, I K Sabree, and Ali H S Abd. 2021. "An Examination of the Effect of Adding Zirconia to Bioactive Glass-Ceramic Properties." *IOP Conference Series: Materials Science and Engineering* 1067(1): 012121.
- Dang, Tan Hiep et al. 2020. "Characterization of Bioactive Glass Synthesized by Sol-Gel Process in Hot Water." 5: 1–10.
- Fernandes, Hugo R. et al. 2018. "Bioactive Glasses and Glass-Ceramics for Healthcare Applications in Bone Regeneration and Tissue Engineering." *Materials* 11(12): 1–54.
- Gavinho, S. R. et al. 2021. "Structural, Thermal, Morphological and Dielectric Investigations on 45S5 Glass and Glass-Ceramics." *Journal of Non-Crystalline Solids* 562(January): 120780. <https://doi.org/10.1016/j.jnoncrysol.2021.120780>.
- Gmeiner, R. et al. 2015. "Additive Manufacturing of Bioactive Glasses and Silicate Bioceramics." *Journal of Ceramic Science and Technology* 6(2): 75–86.
- Kaur, Gurbinder et al. 2019. "Mechanical Properties of Bioactive Glasses, Ceramics, Glass-Ceramics and Composites: State-of-the-Art Review and Future Challenges." *Materials Science and Engineering C* 104(December 2018): 109895. <https://doi.org/10.1016/j.msec.2019.109895>.
- Kolli, Nishant Kumar, Sai Phalguna Kanikaram, et al. 2022. "Exploring the Potential Structural, Optical, Dielectric Facets and in-Vitro Behavior of Combeite Synthesized by the Sol-Gel Route." *Physica Scripta* 97(7).
- Kolli, Nishant Kumar, Datta Darshan V M, et al. 2022. "Probing into the Potential Features of Sodium Calcium Silicate (Na<sub>2</sub>Ca<sub>2</sub>Si<sub>3</sub>O<sub>9</sub>) Synthesized by the Solid-State Route." *Physica Scripta* 97(8).
- Kumar, Sanjeet. "Bioactive Glass Ceramics Using Rice Husk Ash Waste Material by DEPARTMENT OF CERAMIC ENGINEERING."
- Mezahi, Fatima-zohra et al. 2018. "Reactivity Kinetics of Sol-Gel Derived 52S4 Glass versus the Treatment Temperature To Cite This Version : HAL Id : Hal-01915389."
- Mirza, Ambreen et al. 2017. "Effect of Temperature on Mechanical and Bioactive Properties of Glass-Ceramics." *Journal of Alloys and Compounds* 726: 348–51. <http://dx.doi.org/10.1016/j.jallcom.2017.07.285>.
- Patternson, A.L. 1939. "Scherrer Formula.Pdf." *Physical review* 56: 978.
- Quintero Sierra, Lindsey Alejandra, and Diana Marcela Escobar. 2019. "Characterization and Bioactivity Behavior of Sol-Gel Derived Bioactive Vitroceramic from Non-Conventional Precursors." *Boletín de la Sociedad Espanola de Ceramica y Vidrio* 58(2): 85–92.
- Zaid, M. H.M. et al. 2020. "Synthesis and Characterization of Samarium Doped Calcium Soda-Lime-Silicate Glass Derived Wollastonite Glass-Ceramics." *Journal of Materials Research and Technology* 9(6): 13153–60. <https://doi.org/10.1016/j.jmrt.2020.09.058>.
- Zosiamliana, R. et al. 2022. "Electronic, Mechanical, Optical and Piezoelectric Properties of Glass-like Sodium Silicate (Na<sub>2</sub>SiO<sub>3</sub>) under Compressive Pressure." *RSC Advances* 12(20): 12453–62.